

Inclusive J/ψ photoproduction and polarization at HERA in the k_T -factorization approach

S.P. Baranov^a, A.V. Lipatov^b, N.P. Zotov^b

October 23, 2018

^a *P.N. Lebedev Physics Institute,
119991 Moscow, Russia*

^b *D.V. Skobeltsyn Institute of Nuclear Physics,
M.V. Lomonosov Moscow State University,
119991 Moscow, Russia*

Abstract

We investigate the inclusive photoproduction of J/ψ mesons at HERA within the framework of the k_T -factorization QCD approach. Our consideration is based on the color singlet model supplemented with the relevant off-shell matrix elements and the CCFM and KMR unintegrated gluon densities in a proton and in a photon. Both the direct and resolved photon contributions are taken into account. Our predictions are compared with the recent experimental data taken by the H1 and ZEUS collaborations. Special attention is put on the J/ψ polarization parameters λ and ν which are sensitive to the production dynamics.

PACS number(s): 12.38.-t, 13.85.-t

1 Introduction

Heavy quarkonium production at high energies is subject of intense study from both theoretical and experimental points of view [1–3]. The puzzling history traces back to the early 1990s, when the measurements of the J/ψ and Υ hadroproduction cross sections at Tevatron energies revealed a more than one order-of-magnitude discrepancy with the theoretical expectations of the color singlet (CS) model [4]. This fact has induced extensive theoretical activity, mainly in the description of the formation of bound $q\bar{q}$ state from the heavy quark pair produced in the hard interaction (photon-gluon or gluon-gluon fusion). In the CS model, only those states with the same quantum numbers as the resulting quarkonium contribute to the formation of

a bound state. This is achieved by radiating a hard gluon in a perturbative process. In the color octet (CO) model [5], it was suggested to add the contribution of transition mechanism from $q\bar{q}$ pairs to quarkonium, where a heavy quark pair is produced in a color octet state and transforms into the final color singlet state by the help of soft gluon radiation. The CO model is based on the general principle of the non-relativistic QCD factorization (NRQCD) [6]. By adding the contribution from the octet states and fitting the free parameters one was able to describe the existing data on the J/ψ and Υ production at the Tevatron [7].

However, recently the NLO QCD corrections to CS mechanism have been found to be essential in quarkonium production [8]. The large discrepancies between experiments and LO CS predictions for J/ψ and Υ inclusive production can be largely resolved at NLO level within the CS model [8,9]. These NLO corrections to the J/ψ production at the Tevatron enhance the cross section at large p_T by two orders of magnitude [9,10]. The complete NLO calculations of the J/ψ photoproduction at HERA slightly favor the presence of CO contributions [11,12]. In order to achieve agreement between the last calculations and the experimental data for the p_T -distributions measured at HERA and Tevatron the contribution of CO P-wave state to be assumed is negative [12,13]. Another problem refers to the quarkonium spin alignment: the CO model predicts the strong transverse polarization of the produced mesons (see [1]). This is in disagreement with the data which point to unpolarized or even longitudinally polarized quarkoniums [14,15].

A different strategy is represented by the k_T -factorization approach of QCD [16]. This approach is based on the Balitsky-Fadin-Kuraev-Lipatov (BFKL) [17] or Ciafaloni-Catani-Fiorani-Marchesini (CCFM) [18] evolution equations for non-collinear gluon densities in a proton or photon. A detailed description and discussion of the k_T -factorization approach can be found, for example, in reviews [19]. Quarkonium production and polarization have own story in the k_T -factorization approach. Shortly, it was demonstrated [20–24] that in the framework of this approach the experimental data on the heavy quarkonium production at HERA, RHIC and Tevatron can be reasonable well described without the CO contributions. It is important also that the k_T -factorization predicts the longitudinal polarization of J/ψ and Υ mesons as an immediate consequence of initial gluon off-shellness [25]. The results of recent theoretical calculations of the NLO and NNLO corrections to CS quarkonium production in the framework of standard pQCD [8,9] are in much better agreement with the k_T -factorization predictions [20–24] than it was seen for LO collinear calculations.

The present note is motivated by the very recent experimental measurements [26,27] of the inclusive J/ψ photoproduction cross sections performed by the H1 and ZEUS collaborations at HERA. These measurements have been performed with increased statistics and precision as compared with previous experimental analyses [28,29]. The number of single and double differential cross sections are determined and the polarisation parameters λ and ν are measured in the several different reference frames (namely helicity, target and Collins-Soper frames) as a function of J/ψ transverse momentum and elasticity variable z . Our main goal is to give a systematic analysis of available experimental data [26–29] in the framework of the CS model and the k_T -factorization approach supplemented with the CCFM gluon dynamics, what we not done in our first paper [20]. In this analysis we will take into account both direct and resolved photon contributions (last of them are important at low z). Specially we concentrate on the J/ψ polarization observables since it can be useful, in particular, in discriminating the CS and CO production mechanisms. Also we will study the possible sources of theoretical

uncertainties of our predictions (i.e. uncertainties connected with the gluon evolution scheme and hard scale of partonic subprocess). To investigate the dependence of our predictions on the non-collinear evolution scheme we will apply the unintegrated gluon densities derived from the usual (i.e. DGLAP-evolved) parton distributions (in the Kimber-Martin-Ryskin (KMR) [30] approximation).

The outline of our paper is following. In Section 2 we recall shortly the basic formulas of the k_T -factorization approach with a brief review of calculation steps. In Section 3 we present the numerical results of our calculations and a discussion. Section 4 contains our conclusions.

2 Theoretical framework

In the present note we follow the approach described in detail in our previous paper [20]. Here we only briefly recall the basic formulas.

In the framework of the CS model, the production of any heavy quarkonium is described as the perturbative production of a color singlet quark-antiquark pair in a state with properly arranged the quantum numbers, according to the quarkonium state under consideration. Our calculations in the k_T -factorization approach are based on the off-shell (k_T -dependent) photon-gluon and gluon-gluon fusion subprocesses $\gamma g^* \rightarrow J/\psi g$ and $g^* g^* \rightarrow J/\psi g$. The spin projection operator [4]

$$J(p_\psi) = \hat{\epsilon}_\psi(\hat{p}_\psi + m_\psi)/2m_\psi, \quad (1)$$

is included to guarantee the proper quantum numbers of the created charmed quark pair. Here m_ψ , p_ψ and ϵ_ψ are the mass, four-momentum and polarization vectors of produced J/ψ . In accordance with the non-relativistic formalism of bound state formation, the charmed quarks are assumed to each carry one half of the J/ψ momentum and the probability of creation of J/ψ meson is determined by a value of wave function at the origin of coordinate space $|\Psi(0)|^2$, which is known from the leptonic decay width [31]. The calculation of relevant off-shell matrix elements $|\bar{\mathcal{M}}(\gamma g^* \rightarrow J/\psi g)|^2$ and $|\bar{\mathcal{M}}(g^* g^* \rightarrow J/\psi g)|^2$ has been described detally in [20]. Here we would like to only mention two technical points. First, in according to the k_T -factorization prescription [16], the summation over the incoming off-shell gluon polarizations is carried with $\sum \epsilon^\mu \epsilon^{*\nu} = \mathbf{k}_T^\mu \mathbf{k}_T^\nu / \mathbf{k}_T^2$, where \mathbf{k}_T is the gluon transverse momentum. Second, the spin density matrix of J/ψ meson is determined by the momenta l_1 and l_2 of the decay leptons and is taken in the form¹

$$\sum \epsilon_\psi^\mu \epsilon_\psi^{*\nu} = 3 \left(l_1^\mu l_2^\nu + l_1^\nu l_2^\mu - \frac{m_\psi^2}{2} g^{\mu\nu} \right) / m_\psi^2. \quad (2)$$

This expression is equivalent to the standard one $\sum \epsilon_\psi^\mu \epsilon_\psi^{*\nu} = -g^{\mu\nu} + p_\psi^\mu p_\psi^\nu / m_\psi^2$ (which has been used previously in [20, 21]) but is better suited for studying the polarization variables.

The cross section of J/ψ photoproduction at high energies in the k_T -factorization approach is calculated as a convolution of the off-shell partonic cross section $\hat{\sigma}$ and the unintegrated gluon distributions in a proton and in a photon. The direct and resolved photon contributions

¹This formula has misprint in [22].

can be presented in the following form:

$$\begin{aligned} \sigma_{\text{dir}}(\gamma p \rightarrow J/\psi X) &= \int \frac{1}{16\pi(x_2 W^2)^2} \frac{1}{z(1-z)} \mathcal{A}(x_2, \mathbf{k}_{2T}^2, \mu^2) \times \\ &\times |\bar{\mathcal{M}}(\gamma g^* \rightarrow J/\psi g)|^2 d\mathbf{p}_{\psi T}^2 d\mathbf{k}_{2T}^2 dz \frac{d\phi_2}{2\pi}, \end{aligned} \quad (3)$$

$$\begin{aligned} \sigma_{\text{res}}(\gamma p \rightarrow J/\psi X) &= \int \frac{1}{16\pi(x_1 x_2 W^2)^2} \mathcal{A}_\gamma(x_1, \mathbf{k}_{1T}^2, \mu^2) \mathcal{A}(x_2, \mathbf{k}_{2T}^2, \mu^2) \times \\ &\times |\bar{\mathcal{M}}(g^* g^* \rightarrow J/\psi g)|^2 d\mathbf{p}_{\psi T}^2 d\mathbf{k}_{1T}^2 d\mathbf{k}_{2T}^2 dy_\psi dy_g \frac{d\phi_1}{2\pi} \frac{d\phi_2}{2\pi}, \end{aligned} \quad (4)$$

where $\mathcal{A}(x, \mathbf{k}_T^2, \mu^2)$ and $\mathcal{A}_\gamma(x, \mathbf{k}_T^2, \mu^2)$ are the unintegrated gluon distributions in a proton and in a photon, y_ψ and y_g are the rapidities of produced J/ψ meson and outgoing gluon and W is the photon-proton center-of-mass energy. The initial off-shell gluons have a fraction x_1 and x_2 of the parent proton and photon longitudinal momenta, non-zero transverse momenta \mathbf{k}_{1T} and \mathbf{k}_{2T} ($\mathbf{k}_{1T}^2 = -k_{1T}^2 \neq 0$, $\mathbf{k}_{2T}^2 = -k_{2T}^2 \neq 0$) and azimuthal angles ϕ_1 and ϕ_2 . The elasticity z denotes the fractional energy of the photon transferred to the J/ψ meson in the proton rest system: $z = (p_\psi \cdot p_p)/(p_\gamma \cdot p_p)$, where p_γ and p_p are the four-momenta of the incoming photon and proton.

The unintegrated gluon distributions in a proton and in a photon involved in (3) and (4) can be obtained from the analytical or numerical solutions of the BFKL or CCFM evolution equations. In the numerical calculations we have tested a few different sets. First of them, unintegrated gluon density in a proton (CCFM set A0) has been obtained in [32] from the CCFM equation where all input parameters have been fitted to describe the proton structure function $F_2(x, Q^2)$. Equally good fit was obtained using different values for the soft cut and a different value for the width of the intrinsic \mathbf{k}_T distribution (CCFM set B0). A reasonable description of the F_2 data can be achieved [32] by both A0 and B0 sets. These unintegrated gluon densities in a proton will be supplemented with the CCFM-evolved gluon density in a photon proposed in [33]. Also we will use the unintegrated gluon densities in a proton and in a photon taken in the Kimber-Martin-Ryskin form [30]. The KMR approach is a formalism to construct the unintegrated parton distributions from well-known conventional ones. For the input, we have used the leading-order GRV parametrizations [34].

The multidimensional integrations in (3) and (4) have been performed by the means of Monte Carlo technique, using the routine VEGAS [35]. The full C++ code is available from the authors on request².

3 Numerical results

We now are in a position to present our numerical results. First we describe our input and the kinematic conditions. After we fixed the unintegrated gluon distributions, the cross sections (3) and (4) depend on the renormalization and factorization scales μ_R and μ_F . In the numerical calculations we set $\mu_R = \xi \sqrt{m_\psi^2 + \mathbf{p}_{\psi T}^2}$, $\mu_F = \xi \sqrt{\hat{s} + \mathbf{Q}_T^2}$, where \mathbf{Q}_T is the transverse momentum of initial off-shell gluon or gluon pair (in the case of resolved photon production). In order to

²lipatov@theory.sinp.msu.ru

estimate the theoretical uncertainties of our calculations we vary the scale parameter ξ between 1/2 and 2 about the default value $\xi = 1$. The sensitivity of the predictions to the charmed quark mass has been investigated previously in [20,21]. Here we set $m_c = 1.5$ GeV and use the LO formula for the coupling constant $\alpha_s(\mu^2)$ with $n_f = 4$ quark flavours at $\Lambda_{\text{QCD}} = 200$ MeV, such that $\alpha_s(M_Z^2) = 0.1232$. Note that we apply another value $\Lambda_{\text{QCD}} = 220$ MeV for the CCFM-evolved gluon densities (see discussion in Sect. 3.1). Finally, the J/ψ wave function at the origin of coordinate space is taken to be equal to $|\Psi(0)|^2 = 0.0876$ GeV³ [31].

3.1 Inclusive production

Experimental data for the inclusive J/ψ photoproduction at HERA come from both the ZEUS and H1 collaborations. The dependence of the total cross section on the photon-proton center-of-mass energy W has been measured and the number of single and double differential cross sections has been determined: $d\sigma/dz$, $d\sigma/d\mathbf{p}_{\psi T}^2$, $d\sigma/dy_\psi$ and $d\sigma/d\mathbf{p}_{\psi T}^2 dz$. The ZEUS data [29] refer to the kinematic region defined by $0.1 < z < 0.9$, $\mathbf{p}_{\psi T}^2 > 1$ GeV² and $50 < W < 180$ GeV. The H1 data [28] refer to the kinematic region $0.05 < z < 0.9$, $1 < \mathbf{p}_{\psi T}^2 < 60$ GeV² and $60 < W < 260$ GeV. Very recent H1 measurements [27] have been performed at $0.3 < z < 0.9$, $1 < \mathbf{p}_{\psi T}^2 < 100$ GeV² and $60 < W < 240$ GeV.

Our numerical predictions are shown in Figs. 1 — 7 in comparison with the data [27–29]. The solid, dotted and dash-dotted histograms correspond to the results obtained using the CCFM A0, B0 and KMR gluon densities, respectively. The upper and lower dashed histograms represent the scale variations as it was described above. To estimate this uncertainty we used the CCFM set A0+ and A0– instead of the default gluon density A0: the A0– stands for $\xi = 1/2$ while set A0+ reflects $\xi = 2$. One can see a good overall agreement of our central CCFM predictions with the recent H1 data [27]. We would like to point out that the shape of z distributions is well reproduced by the CS mechanism. It is in a contrast with the predictions [12] where the octet contributions have been taken into account. The transverse momentum distributions and the dependence of J/ψ total cross section on the energy W are well described also. It seems that the agreement of our CCFM predictions with the previous H1 data [28] is slightly less satisfactory but still reasonable (see Figs. 4 — 6). Main difference between data and theory occurs in the high $\mathbf{p}_{\psi T}$ region. We note, however, that the measurements [27,28] have been performed in essentially the same kinematical region and therefore probably there exists a problem of incompatibility of these data with each other. The shape of y_ψ distribution measured by ZEUS is not fully reproduced, but the data points lie still within the band of theoretical uncertainties. In general, the overall agreement of our CCFM predictions with ZEUS data [29] is reasonable well (see Fig. 7). The KMR gluon density is also responsible for description of the H1 and ZEUS data although the shape of W -dependence of J/ψ total cross section is not reproduced well.

The predictions of the Monte Carlo event generator CASCADE [36] have been obtained in the kinematical range of recent H1 measurements [27]. CASCADE is a full hadron level event generator which uses the CCFM equation for the initial state gluon evolution. Despite the fact that the default sets of numerical parameters are the same, the CASCADE predictions (based on the A0 gluon density) lie somewhat above than ours. The possible reason can be connected with the corrections for contributions from the non-resonant background events which have been included into the CASCADE calculations (see more details in [27]). These corrections are

not taken into account in our consideration. In addition, there are some effects from the final-state parton showers in CASCADE which are also absent in our approach. However, we obtain the same results as coming from CASCADE if we apply the small shift in QCD parameter to $\Lambda_{\text{QCD}} = 220$ MeV. This is the reason why such shifted value of Λ_{QCD} has been used in our CCFM calculations. In this way we effectively simulate the missing final-state parton showers effects and effects coming from non-resonant background events. It leads to increase of the predicted cross sections by the 15% approximately, that is, of course, much less than the scale uncertainties of our calculations. Note that the choice $\Lambda_{\text{QCD}} = 200$ MeV in the KMR predictions is defined by the set of relevant parameters in GRV parametrizations.

3.2 Polarization properties

Now we turn now to the investigation of the J/ψ polarization in photoproduction events at HERA. As it was mentioned above, the polarization observables are useful in discriminating the CS and CO production mechanisms, as well as collinear and k_T -factorization approaches. In general, the spin density matrix of a vector particle depends on three parameters λ , μ and ν which can be measured experimentally from the double differential angular distribution of the decay products. The latter reads for the J/ψ leptonic decay [37]

$$\frac{d\sigma}{d\phi^* d\cos\theta^*} \sim 1 + \lambda \cos^2\theta^* + \mu \sin 2\theta^* \cos\phi^* + \frac{\nu}{2} \sin^2\theta^* \cos 2\phi^*, \quad (5)$$

where θ^* and ϕ^* are the polar and azimuthal angles of the decay lepton measured in the J/ψ rest frame. In the H1 experiments [27, 28] the polarization parameters λ and ν have been measured as a functions of $\mathbf{p}_{\psi T}$ and z in two complementary frames: the helicity frame and Collins-Soper frame. In addition, the ZEUS collaboration performs the measurements in the target frame [26, 29]. In the helicity frame the polarization axis in the J/ψ meson rest frame is defined by the flight direction of the J/ψ meson in the γp rest frame, whereas the polarization in the Collins-Soper frame is measured with respect to the bisector of proton ($-\vec{p}_p$) and photon (\vec{p}_γ) in the J/ψ meson rest frame. In the target frame the polarization axis is chosen to be opposite of the incoming proton direction in the J/ψ rest frame. Note that cases $\lambda = 1$ and $\lambda = -1$ correspond to transverse and longitudinal polarization of the J/ψ meson, respectively. Unfortunately, the experimental statistics was insufficient to encourage the extraction of parameter μ from the double differential cross section (5). Our theoretical calculations were adjusted to the experimental binning and generally followed the experimental procedure. We have collected the simulated events in the specified bins of $p_{\psi T}$ and z , generated the decay lepton angular distributions according to the production and decay matrix elements, and then applied a three-parametric fit based on (5).

The estimated values of λ and ν are shown in Figs. 8 — 15 in comparison with the H1 [27, 28] and ZEUS experimental data [26, 29]. The solid and dash-dotted histograms represent the results obtained in the k_T -factorization approach with the CCFM A0 and KMR gluon densities. The dotted histograms correspond to the LO CS model predictions. First of all, one can clearly see the difference between the collinear and k_T -factorization approaches in behavior of parameter λ as a function of $p_{\psi T}$. In contrast with the LO CS model, the k_T -factorization predicts the longitudinal polarization of produced J/ψ mesons at high transverse momenta. Note that if the NLO corrections to the LO CS cross section will be taken into account, the

J/ψ polarization is also tends to be longitudinal [8]. It is not the case of CO predictions where NLO corrections keep the essential transverse polarization. The parameter λ as a function of z seems to be insufficient to discriminate between the two production mechanisms. Contrary, behaviour of parameter ν as a function of z demonstrates the analyzing power and can be useful to distinguish both the approaches.

Concerning the comparison of our predictions and the data, one can see that none of the predictions can describe all aspects of the data even though huge experimental uncertainties. However, the k_T -factorization approach tends to be in a better agreement with the data, especially with respect to the $p_{\psi T}$ dependence of λ and z dependence of ν . We point out that our predictions for the polarization parameters λ and ν are not sensitive to the unintegrated gluon density used. So one of the sources of theoretical uncertainties is cancels out. Therefore measurements of the polarization parameters can to play crucial role in discriminating the different theoretical approaches.

4 Conclusions

We have studied inclusive J/ψ meson photoproduction at HERA within the framework of the k_T -factorization approach. Our consideration is based on the usual CS model supplemented with the relevant off-shell matrix elements and the CCFM-evolved unintegrated gluon densities in a proton and in a photon. Both the direct and resolved photon contributions are taken into account. The analysis covers the total, single and double differential cross sections of J/ψ mesons. Special attention was put on the polarization parameters λ and ν which determine the J/ψ spin density matrix.

We obtained a reasonable well agreement of our calculations and the recent experimental data taken by the H1 and ZEUS collaborations. We demonstrated that the k_T -factorization approach gives a better agreement with the polarization data than the leading-order collinear calculations. Both polarization parameters λ and ν can be used to discriminate the J/ψ production mechanism and study the parton interaction dynamics.

5 Acknowledgements

The authors are very grateful to DESY Directorate for the support in the framework of Moscow — DESY project on Monte-Carlo implementation for HERA — LHC. A.V.L. was supported in part by the Helmholtz — Russia Joint Research Group. Also this research was supported by the FASI of Russian Federation (grant NS-4142.2010.2) and FASI state contract 02.740.11.0244.

References

- [1] M. Krämer, Prog. Part. Nucl. Phys. **47**, 141 (2001).
- [2] J.P. Lansberg, Int. J. Mod. Phys. A **21**, 3857 (2006).
- [3] N. Brambilla *et al.*, CERN-2005-005; arXiv: hep-ph/0412158.

- [4] C.-H. Chang, Nucl. Phys. B **172**, 425 (1980);
E.L. Berger and D.L. Jones, Phys. Rev. D **23**, 1521 (1981);
R. Baier and R. Rückl, Phys. Lett. B **102**, 364 (1981);
S.S. Gershtein, A.K. Likhoded, and S.R. Slabospitsky, Sov. J. Nucl. Phys. **34**, 128 (1981).
- [5] E. Braaten and S. Fleming, Phys. Rev. Lett. **74**, 3327 (1995).
- [6] G. Bodwin, E. Braaten, and G. Lepage, Phys. Rev. D **51**, 1125 (1995); Phys. Rev. D **55**, 5853 (1997).
- [7] P. Cho and A.K. Leibovich, Phys. Rev. D **53**, 150 (1996); Phys. Rev. D **53**, 6203 (1996).
- [8] P. Artoisenet, J. Campbell, J.P. Lansberg, F. Maltoni, and F. Tramontano, Phys. Rev. Lett. **101**, 152001 (2008).
- [9] B. Gong and J.-X. Wang, Phys. Rev. Lett. **100**, 232001 (2008); Phys. Rev. D **78**, 074011 (2008).
- [10] J.M. Campbell, F. Maltoni, and F. Tramontano, Phys. Rev. Lett. **98**, 252002 (2007).
- [11] P. Artoisenet, J. Campbell, F. Maltoni, and F. Tramontano, Phys. Rev. Lett. **102**, 142001 (2009).
- [12] M. Butenschön and B.A. Kniehl, DESY 10-101; arXiv:1009.5662 [hep-ph].
- [13] Y.-Q. Ma, K. Wang, and K. T Chao, arXiv:1009.3655 [hep-ph].
- [14] D. Acosta *et al.* (CDF Collaboration), Phys. Rev. Lett. **88**, 161802 (2002).
- [15] V.M. Abazov *et al.* (D0 Collaboration), Phys. Rev. Lett. **101**, 182004 (2008).
- [16] L.V. Gribov, E.M. Levin, and M.G. Ryskin, Phys. Rep. **100**, 1 (1983);
E.M. Levin, M.G. Ryskin, Yu.M. Shabelsky and A.G. Shuvaev, Sov. J. Nucl. Phys. **53**, 657 (1991);
S. Catani, M. Ciafaloni and F. Hautmann, Nucl. Phys. B **366**, 135 (1991);
J.C. Collins and R.K. Ellis, Nucl. Phys. B **360**, 3 (1991).
- [17] E.A. Kuraev, L.N. Lipatov and V.S. Fadin, Sov. Phys. JETP **44**, 443 (1976);
E.A. Kuraev, L.N. Lipatov and V.S. Fadin, Sov. Phys. JETP **45**, 199 (1977);
I.I. Balitsky and L.N. Lipatov, Sov. J. Nucl. Phys. **28**, 822 (1978).
- [18] M. Ciafaloni, Nucl. Phys. B **296**, 49 (1988);
S. Catani, F. Fiorani and G. Marchesini, Phys. Lett. B **234**, 339 (1990);
S. Catani, F. Fiorani and G. Marchesini, Nucl. Phys. B **336**, 18 (1990);
G. Marchesini, Nucl. Phys. B **445**, 49 (1995).
- [19] B. Andersson *et al.* (Small- x Collaboration), Eur. Phys. J. C **25**, 77 (2002);
J. Andersen *et al.* (Small- x Collaboration), Eur. Phys. J. C **35**, 67 (2004);
J. Andersen *et al.* (Small- x Collaboration), Eur. Phys. J. C **48**, 53 (2006).

- [20] A.V. Lipatov, N.P. Zotov, Eur. Phys. J. C **27**, 87 (2003).
- [21] S.P. Baranov, N.P. Zotov, J. Phys. G **29**, 1395 (2003).
- [22] S.P. Baranov, Yad. Fiz. **73**, 1 (2010).
- [23] S.P. Baranov, A. Szczurek, Phys. Rev. D **77**, 054016 (2008).
- [24] S.P. Baranov, Phys. Rev. D **66**, 114003 (2002).
- [25] S.P. Baranov, Phys. Lett. B **428**, 377 (1998).
- [26] S. Chekanov *et al.* (ZEUS Collaboration), JHEP **0912**, 007 (2009).
- [27] F.D. Aaron *et al.* (H1 Collaboration), DESY 09-225.
- [28] C. Adloff *et al.* (H1 Collaboration), Eur. Phys. J. C **25**, 25 (2002).
- [29] S. Chekanov *et al.* (ZEUS Collaboration), Eur. Phys. J. C **27**, 173 (2003).
- [30] M.A. Kimber, A.D. Martin and M.G. Ryskin, Phys. Rev. D **63**, 114027 (2001);
G. Watt, A.D. Martin and M.G. Ryskin, Eur. Phys. J. C **31**, 73 (2003).
- [31] C. Amsler *et al.* (PDG Collaboration), Phys. Lett. B **667**, 1 (2008).
- [32] H. Jung, arXiv:hep-ph/0411287.
- [33] M. Hansson, H. Jung, L. Jönsson, arXiv:hep-ph/0402019.
- [34] M. Glück, E. Reya, and A. Vogt, Phys. Rev. D **46**, 1973 (1992);
M. Glück, E. Reya, and A. Vogt, Z. Phys. C **67**, 433 (1995).
- [35] G.P. Lepage, J. Comput. Phys. **27**, 192 (1978).
- [36] H. Jung, Comp. Phys. Comm. **143**, 100 (2002);
H. Jung *et al.*, DESY 10-107.
- [37] M. Beneke, M. Krämer, and M. Vanttinen, Phys. Rev. D **57**, 4258 (1998).

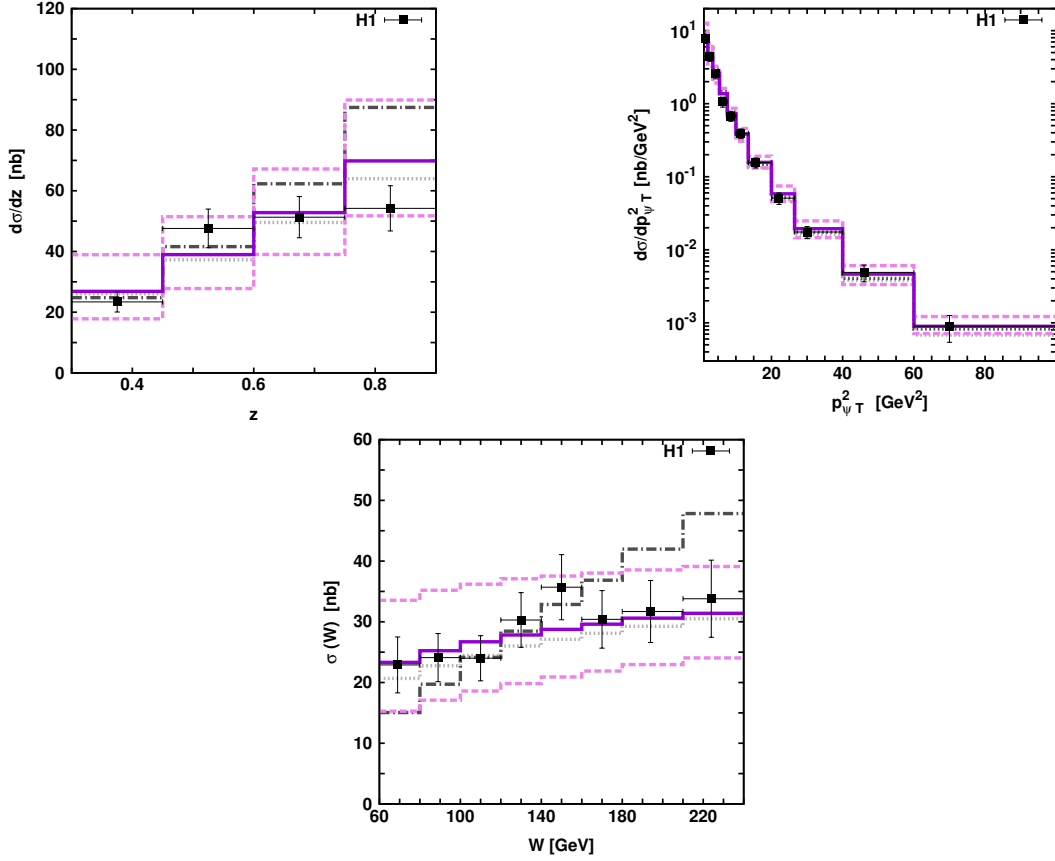


Figure 1: The total and differential cross sections of J/ψ mesons calculated in the kinematical region defined by $0.3 < z < 0.9$, $\mathbf{p}_{\psi T}^2 > 1$ GeV² and $60 < W < 240$ GeV. The solid, dotted and dash-dotted histograms correspond to the results obtained using the CCFM A0, CCFM B0 and KMR gluon densities, respectively. The upper and lower dashed histograms represent the scale scale variations as it is described in the text. The experimental data are from H1 [27].

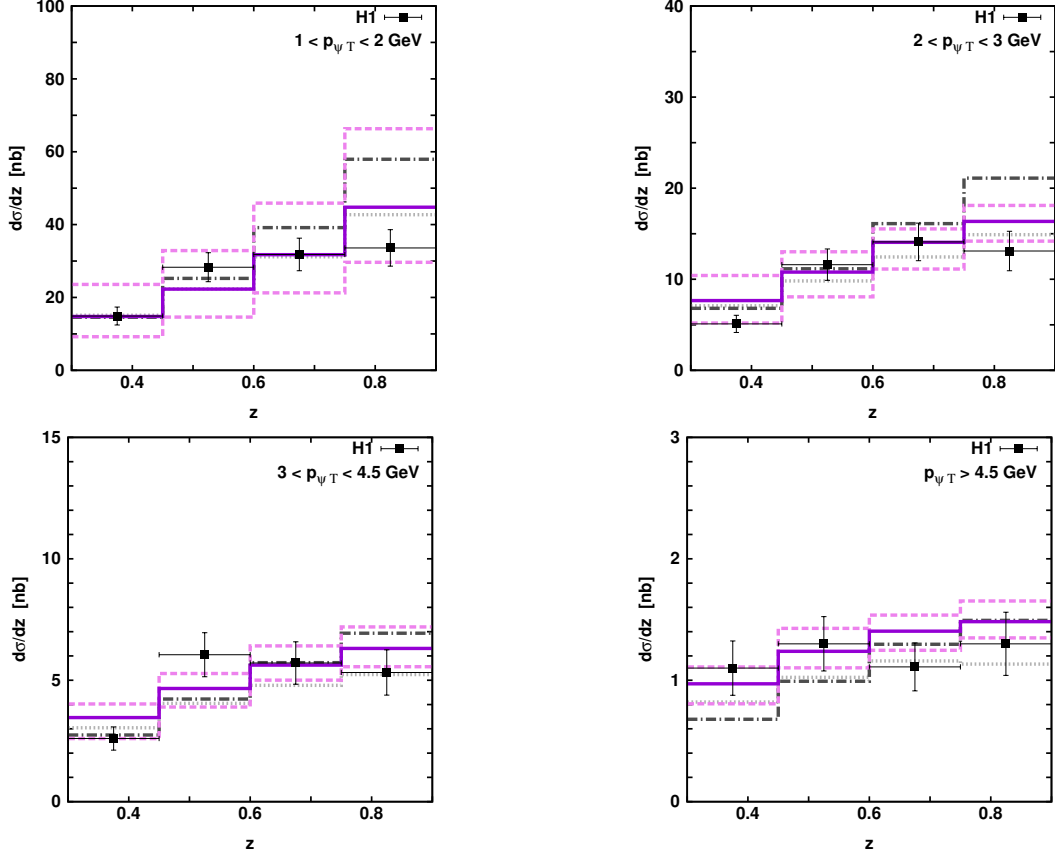


Figure 2: The differential cross sections of J/ψ mesons as a function of elasticity z calculated in different $p_{\psi T}$ bins at $60 < W < 240$ GeV. Notation of all histograms is the same as in Fig. 1. The experimental data are from H1 [27].

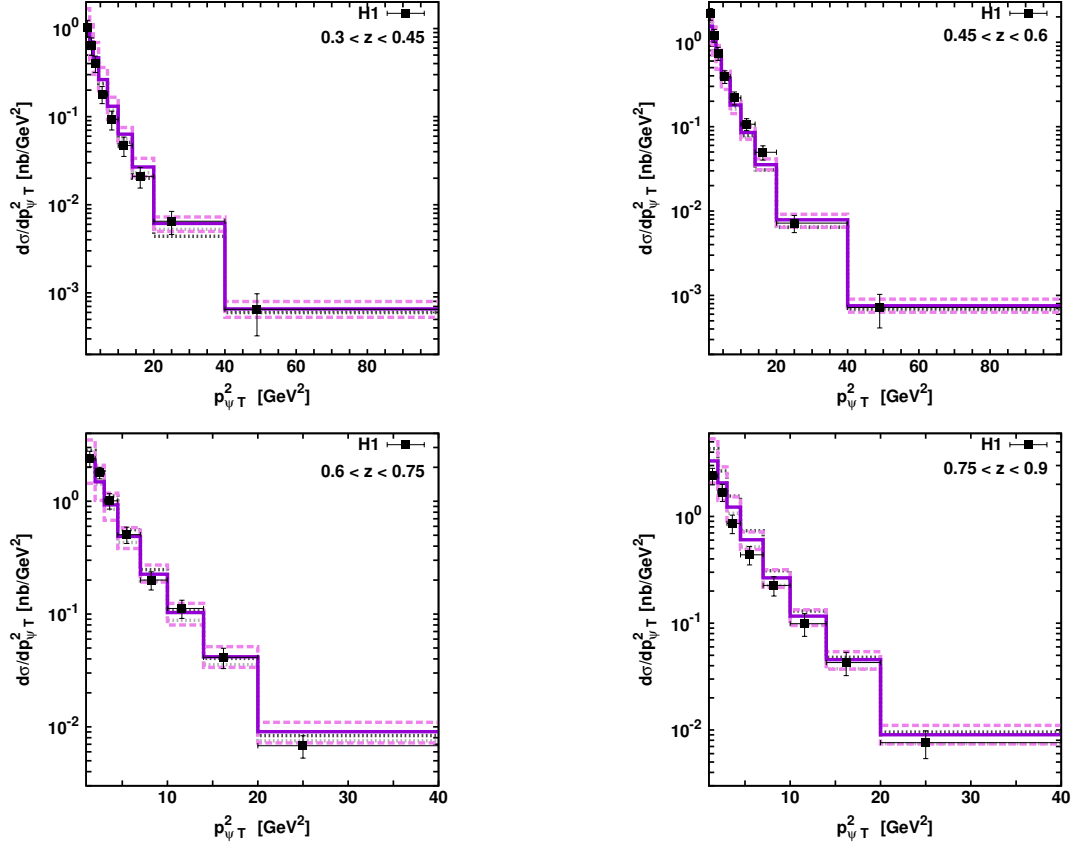


Figure 3: The differential cross sections of J/ψ mesons as a function of $\mathbf{p}_{\psi T}^2$ calculated in different z bins at $60 < W < 240$ GeV. Notation of all histograms is the same as in Fig. 1. The experimental data are from H1 [27].

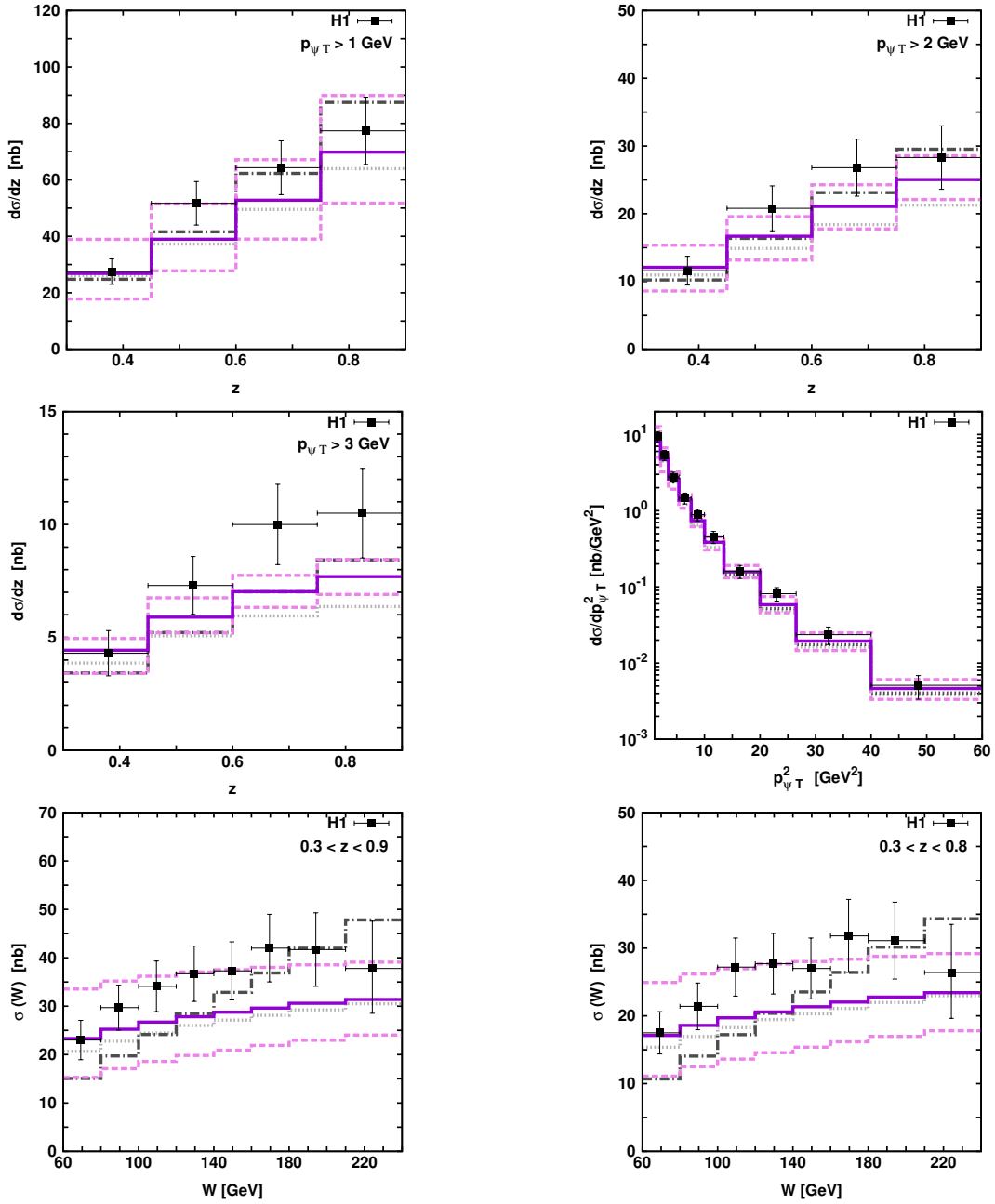


Figure 4: The total and differential cross sections of J/ψ mesons calculated in the kinematical region defined by $0.3 < z < 0.9$, $p_{\psi T}^2 > 1$ GeV² and $60 < W < 240$ GeV. Notation of all histograms is the same as in Fig. 1. The experimental data are from H1 [28].

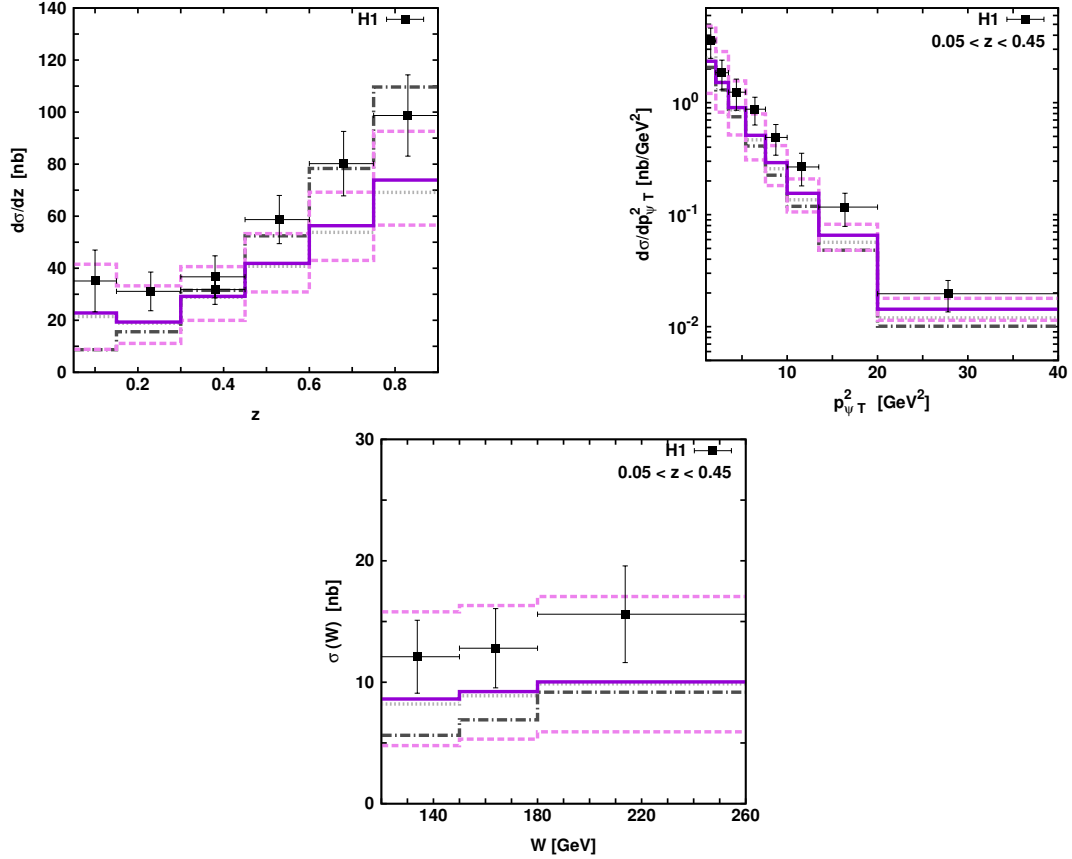


Figure 5: The total and differential cross sections of J/ψ mesons calculated in the kinematical region defined by $0.05 < z < 0.9$, $p_{\psi T}^2 > 1$ GeV 2 and $120 < W < 260$ GeV. Notation of all histograms is the same as in Fig. 1. The experimental data are from H1 [28].

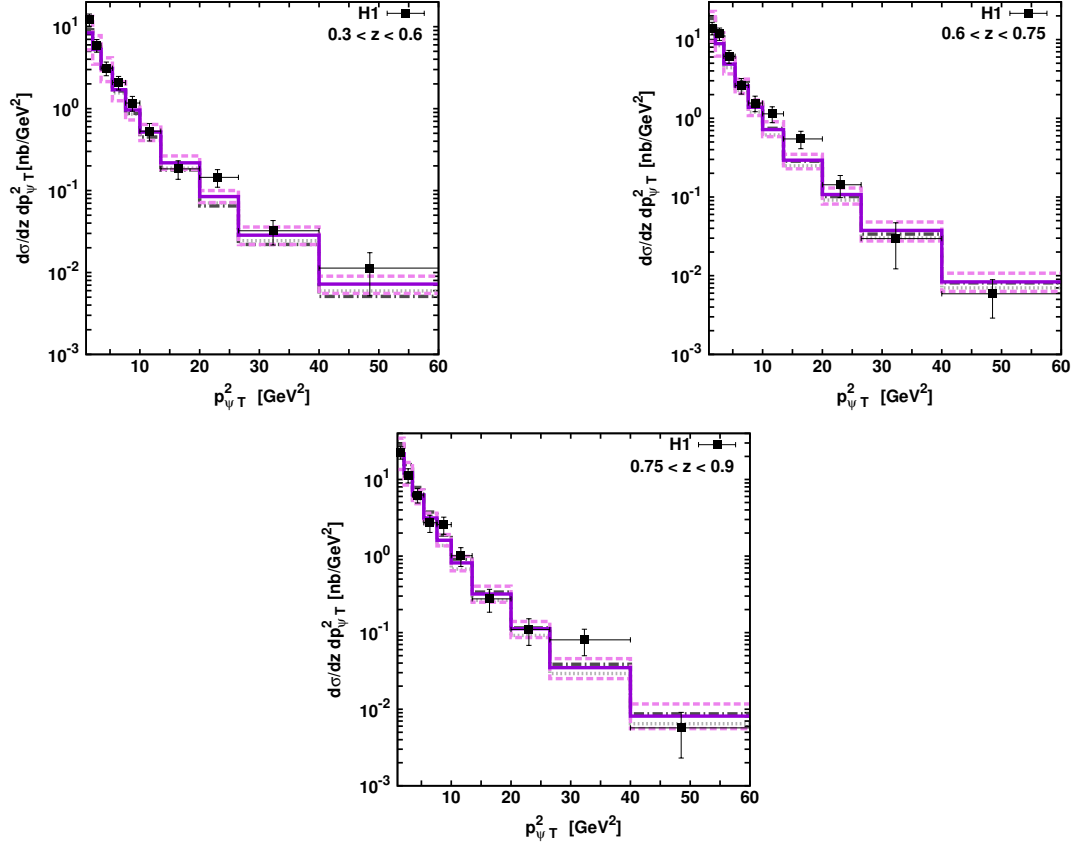


Figure 6: The double differential cross sections of J/ψ mesons in bins of z and $\mathbf{p}_{\psi T}^2$ calculated at $60 < W < 240$ GeV. Notation of all histograms is the same as in Fig. 1. The experimental data are from H1 [28].

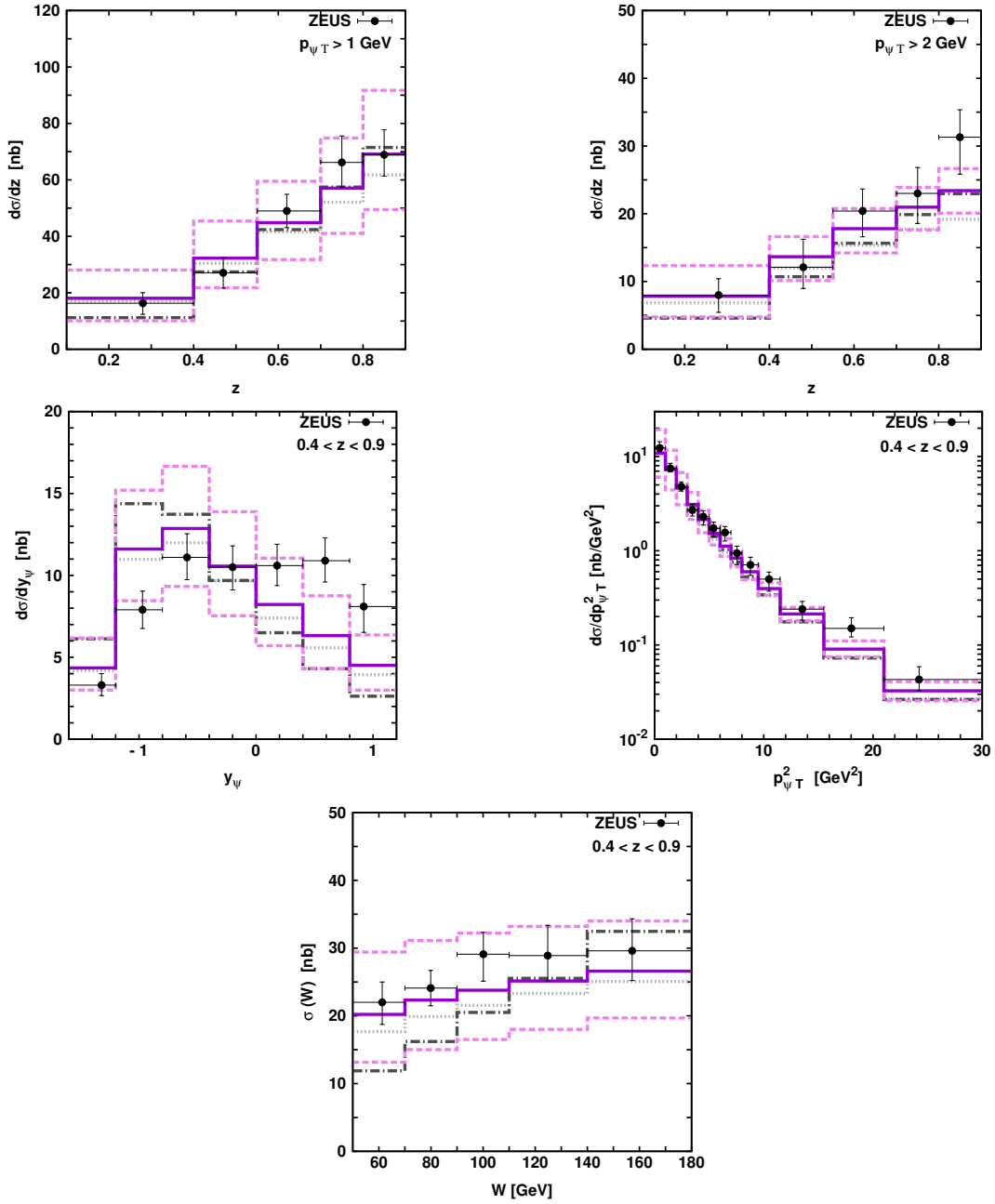


Figure 7: The total and differential cross sections of J/ψ mesons calculated in the kinematical region defined by $0.1 < z < 0.9$, $p_{\psi T}^2 > 1$ GeV² and $50 < W < 180$ GeV. Notation of all histograms is the same as in Fig. 1. The experimental data are from ZEUS [29].

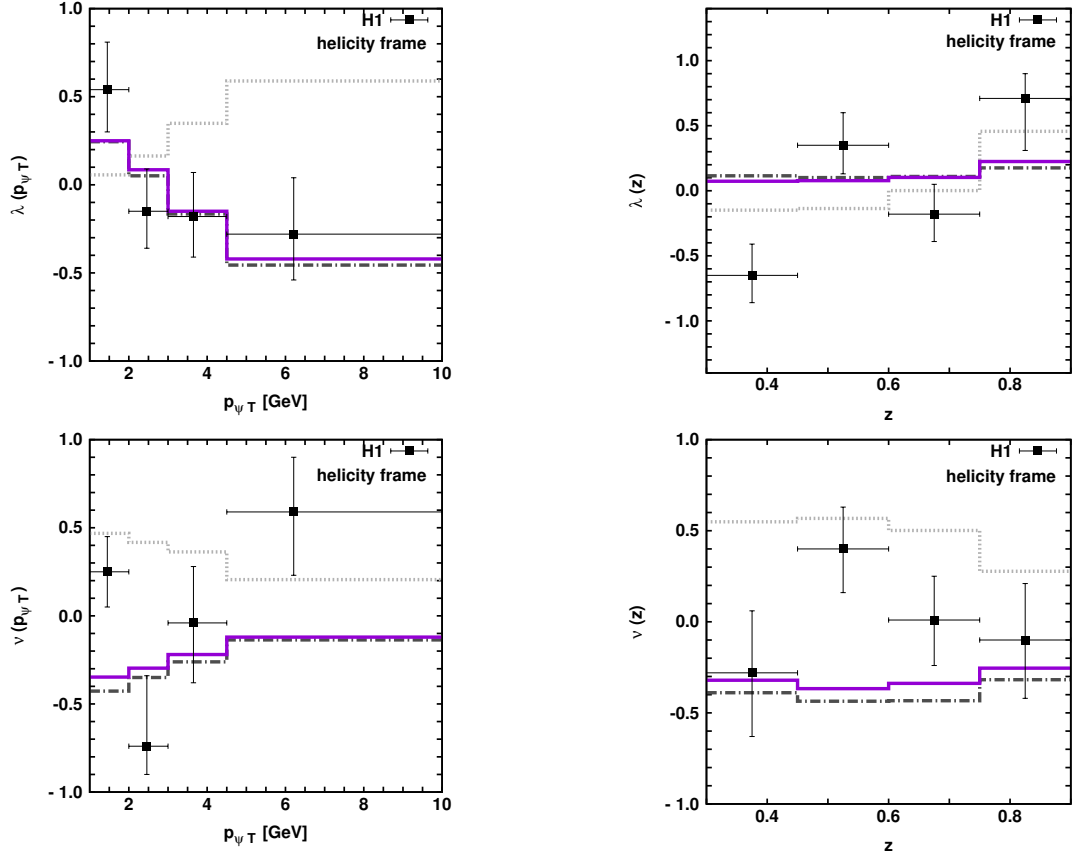


Figure 8: Polarization parameters λ and ν as a functions of the J/ψ transverse momentum and elasticity z calculated in the helicity frame at $0.3 < z < 0.9$, $\mathbf{p}_{\psi T}^2 > 1 \text{ GeV}^2$ and $60 < W < 240 \text{ GeV}$. The solid and dash-dotted histograms correspond to the results obtained using the CCFM A0 and KMR gluon densities. The dotted histograms represent the LO CS predictions. The experimental data are from H1 [27].

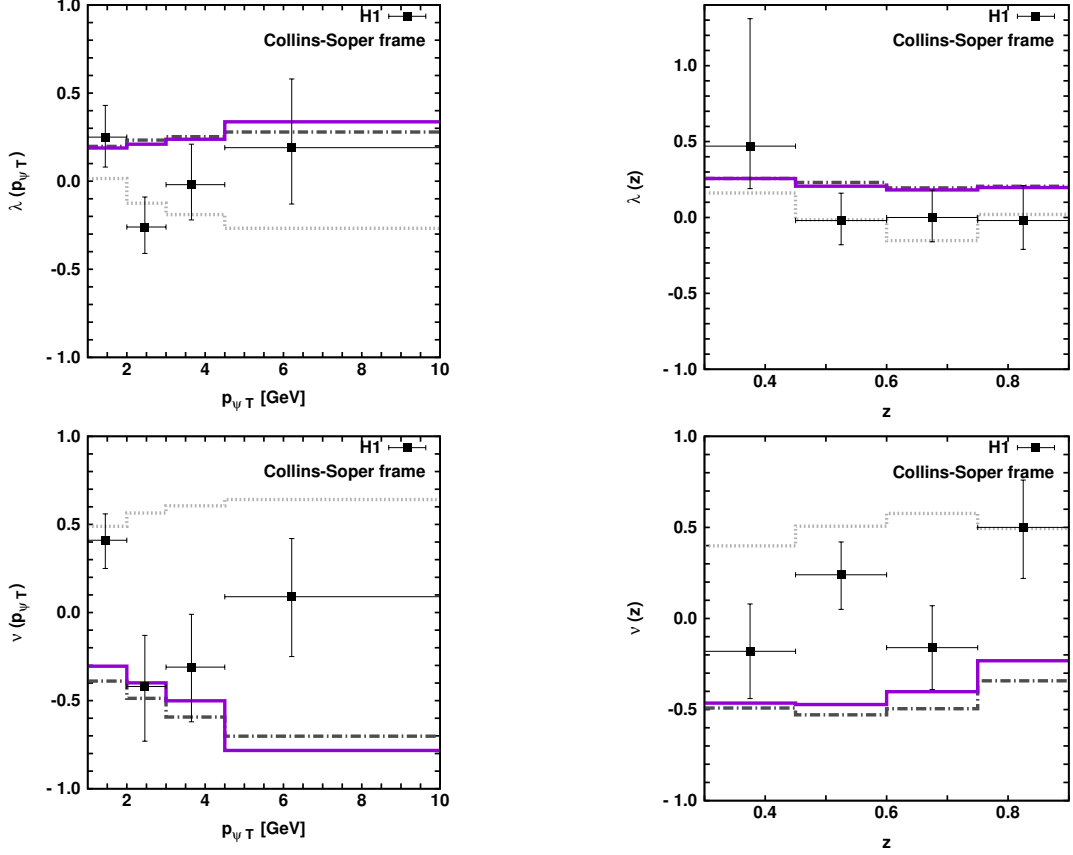


Figure 9: Polarization parameters λ and ν as a functions of the J/ψ transverse momentum and elasticity z calculated in the Collins-Soper frame at $0.3 < z < 0.9$, $\mathbf{p}_{\psi T}^2 > 1 \text{ GeV}^2$ and $60 < W < 240 \text{ GeV}$. Notation of all histograms is the same as in Fig. 8. The experimental data are from H1 [27].

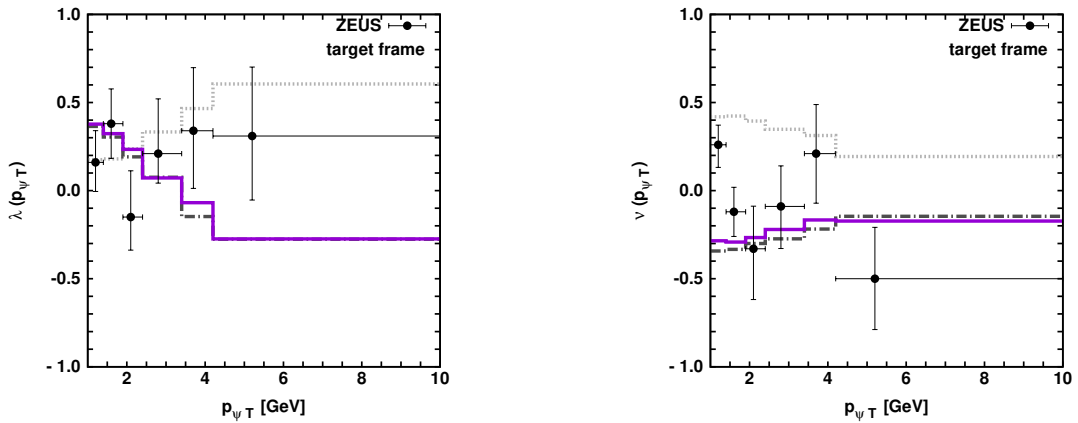


Figure 10: Polarization parameters λ and ν as a functions of the J/ψ transverse momentum calculated in the target frame at $0.4 < z < 1.0$ and $50 < W < 180 \text{ GeV}$. Notation of all histograms is the same as in Fig. 8. The experimental data are from ZEUS [26].

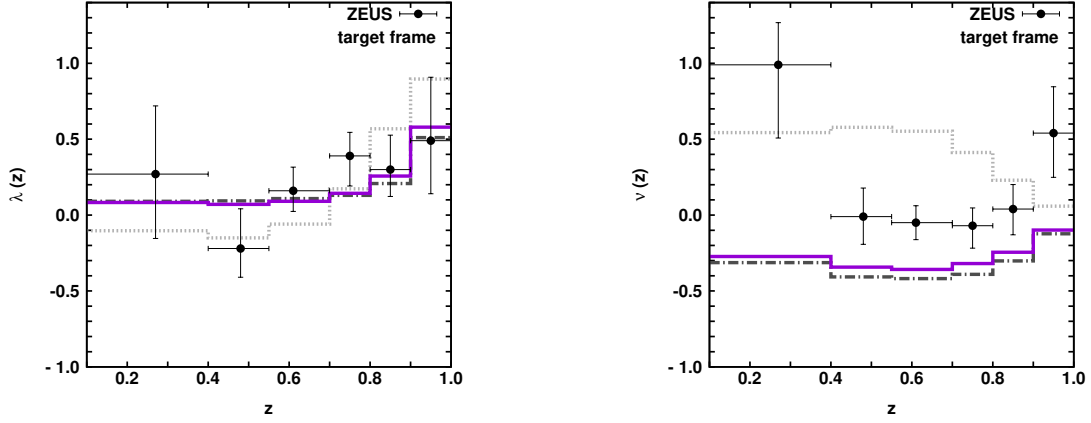


Figure 11: Polarization parameters λ and ν as a functions of the elasticity z calculated in the target frame at $0.1 < z < 1.0$, $p_{\psi T} > 1$ GeV and $50 < W < 180$ GeV. Notation of all histograms is the same as in Fig. 8. The experimental data are from ZEUS [26].

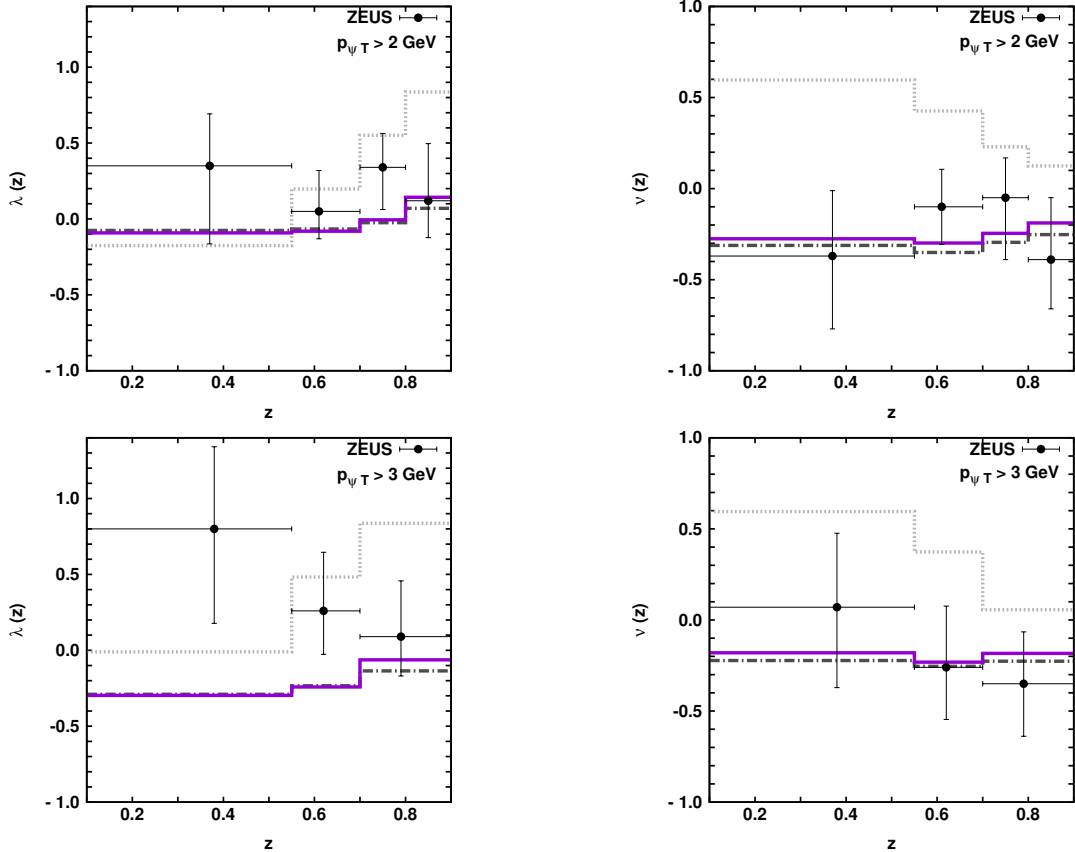


Figure 12: Polarization parameters λ and ν as a functions of the elasticity z calculated in the target frame at $0.1 < z < 0.9$ and $50 < W < 180$ GeV. Notation of all histograms is the same as in Fig. 8. The experimental data are from ZEUS [26].

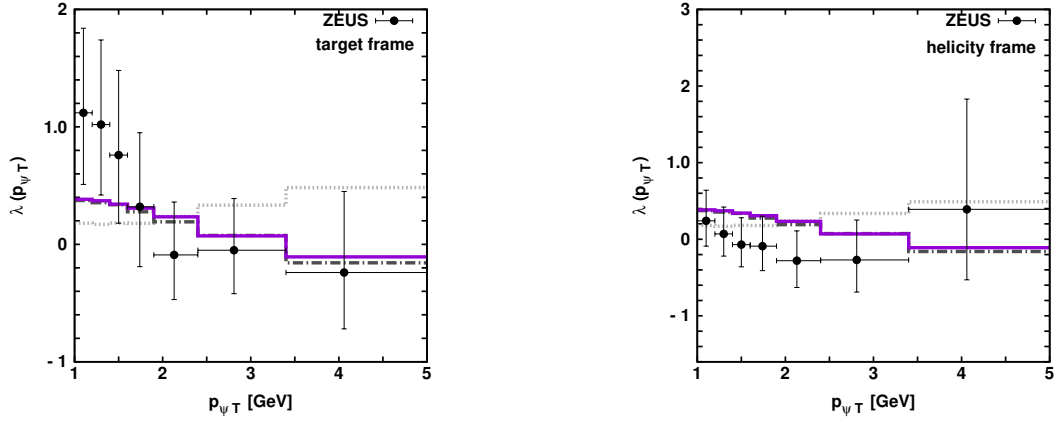


Figure 13: Polarization parameter λ as a function of the J/ψ transverse momentum calculated at $0.4 < z < 1.0$ and $50 < W < 180$ GeV. Notation of all histograms is the same as in Fig. 8. The experimental data are from ZEUS [29].

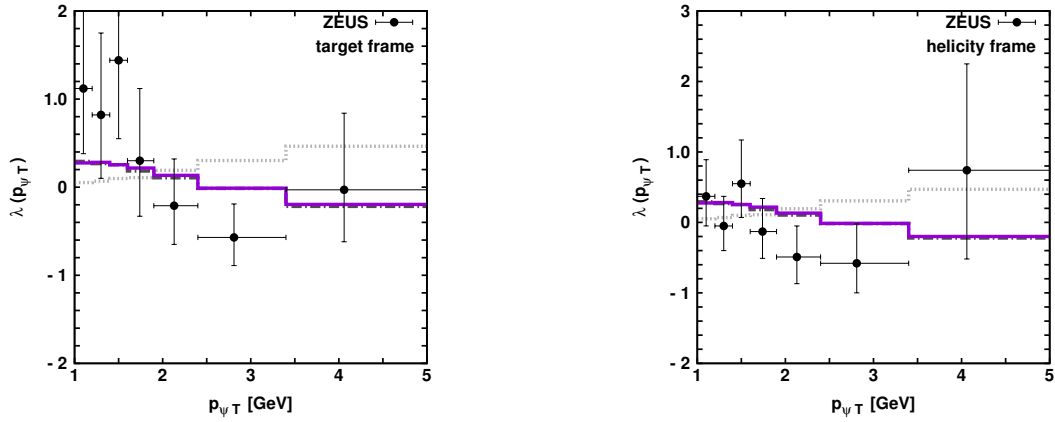


Figure 14: Polarization parameter λ as a function of the J/ψ transverse momentum calculated at $0.4 < z < 0.9$ and $50 < W < 180$ GeV. Notation of all histograms is the same as in Fig. 8. The experimental data are from ZEUS [29].

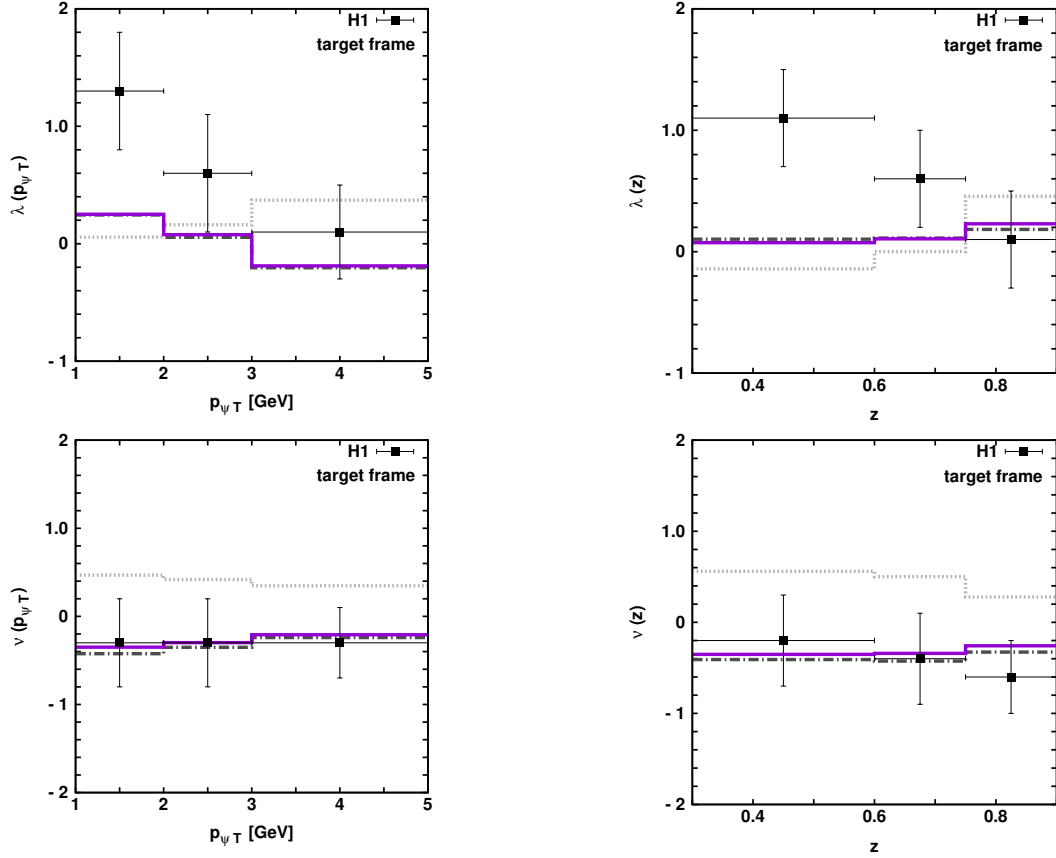


Figure 15: Polarization parameters λ and ν as a functions of the J/ψ transverse momentum and elasticity z calculated in the target frame at $0.3 < z < 0.9$, $\mathbf{p}_{\psi T}^2 > 1 \text{ GeV}^2$ and $60 < W < 240 \text{ GeV}$. Notation of all histograms is the same as in Fig. 8. The experimental data are from H1 [28].